2023

Reactive Atmosphere Pyrolysis(RAP) of Silicon Carbo Nitride (SiCN)

Akshada Bharat Hande

Reactive Atmosphere Pyrolysis (RAP) of Silicon Carbonitride (SiCN) Ceramics

Akshada Hande

Advisor: Peter Kroll

Master Thesis: August 2023

Acknowledgement

I would like to express my heartfelt gratitude to all those who have supported me throughout my Master's thesis journey. This research would not have been possible without the encouragement, guidance, and assistance of numerous individuals. I am deeply indebted to all of them for their invaluable contributions.

First and foremost, I extend my sincere thanks to my research advisor, Dr. Peter Kroll, for their unwavering support and mentorship. Their expertise, patience, and insightful feedback have been instrumental in shaping this thesis. I am immensely grateful for their understanding and support during a crucial period of my life when I embarked on the beautiful journey of motherhood. And I also thank him for guiding me and supporting me while I decided to change the path from pursuing a PhD to Master's degree.

I also want to extend my appreciation to the members of the research committee, Dr. Kwangho Nam, Dr. Macaluso Robin and Dr. Sherri McFarland whose valuable insights and constructive criticism helped refine my work and add depth to my research.

To all my past and current colleagues at Kroll's lab and Dr. John Land, I am grateful for the camaraderie, stimulating discussions, and collaborative spirit that we shared. Your enthusiasm and shared passion for knowledge have been a constant source of inspiration for me.

I express my heartfelt appreciation to Dr. Edwards and Dr. McDougald for their unwavering support and assistance with all our lab needs. Their expertise and dedication have been instrumental in helping us navigate through various challenges, whether it be finding creative instrumentation solutions or directing us to the right resources for any lab-related issues

My heartfelt thanks go out to my dear friends, Dr. Smita Mankar, Dr. Hari Shankar Balakrishnan and Dr. Devaborniny Parasar whose unwavering support and encouragement lifted my spirits during challenging times. Your belief in me, and constant motivation kept me focused on my goals.

I am immensely grateful to my sisters, Dr. Archana Hande-Wajage and Asmita Hande-Sanghavi for their love, encouragement, and understanding. Your presence in my life is a source of strength, and I am thankful for the bond we share.

My journey would have been incomplete without the unwavering support of my parents, Mr. Bharat Hande and Mrs. Vimal Bharat Hande. I am forever grateful to them for instilling in me the value of education and for going above and beyond to support my dreams, even at times challenging societal norms to ensure I had the opportunity to explore all avenues. Their belief in my potential and sacrifices have been the cornerstone of my achievements.

A special mention is also due to my loving husband, Dr. Mikhilesh Dehane, whose unwavering commitment to our family and dedication to taking care of our daughter and other responsibilities allowed me the freedom to focus on my academic pursuits. His constant encouragement and willingness to give his 110% have been an invaluable source of strength, allowing me to reach this milestone.

Lastly, to my precious daughter, Aanandi, thank you for being the light of my life and the driving force behind my perseverance. Your presence has filled my journey with boundless joy and purpose, inspiring me to push my boundaries and achieve more than I thought possible.

I am truly grateful to each and every person mentioned here and to all those who have played a part in my academic and personal journey. Your love, support, and encouragement have been the pillars on which I built my success. Thank you for making this journey worthwhile and for being an integral part of my life.

Abstract

Polymer Derived Ceramics (PDCs) are synthesized by converting liquid polymer precursors into ceramics through controlled pyrolysis. This study focuses on silicon carbonitride (SiCN) ceramics obtained from Ceraset Polysilazane (Durazane1800) precursor. The influence of pyrolysis atmospheres, including inert (Ar, N2) and reactive (H2) environments, on the thermal conversion of Durazane1800 into SiCN ceramics is investigated. The resulting ceramics' chemical variations are explored through phase analysis using X-ray diffraction (XRD), Raman spectroscopy, and thermo gravimetric analysis (TGA). Notably, the impact of hydrogen versus nitrogen atmospheres on the conversion process is analyzed, shedding light on their distinct contributions to the composition and properties of SiCN ceramics. The findings contribute to a comprehensive understanding of PDC synthesis, offering insights into tailoring ceramics for diverse application

Table of Content

Chapter 1: Effect of H_2 atmosphere on the pyrolysis of Durazane 1800 in comparison with N_2 atmosphere

Introduction

Polymer Derived Ceramics (PDCs) are a versatile class of materials that are synthesized through a two-step process involving the processing of liquid polymer precursors at lower temperatures, followed by heat treatments at higher temperatures[1]. This unique approach allows for the fabrication of ceramics with tailored compositions, structures, and properties, opening up a wide range of applications in various fields[2, 3].

The first step in the production of PDCs involves the preparation or selection of liquid polymer precursors[4]. These precursors are typically organic polymers containing elements such as silicon, carbon, nitrogen, and oxygen[2, 5]. Examples of commonly used commercially available precursors include polysilazanes, polyborosilazanes, and polycarbosilanes. The goal of this stage is to form a stable, uniform, and well-defined precursor structure that can be further transformed into a ceramic material. The second step in the PDC production process is the heat treatment of the polymer precursor. This process, known as pyrolysis, transforms the preceramic polymers into ceramics under controlled atmospheres in the furnace. Several factors contribute to the composition and properties of ceramics in Polymer Derived Ceramics (PDCs)[5-7]. The choice of polymer precursor is a crucial factor as different precursors have distinct chemical structures and elemental compositions that influence the composition of the ceramic after pyrolysis.

Additionally, the pyrolysis conditions, such as the heating schedule, temperature ramp rate, and holding times, play a significant role in determining the composition and structure of the ceramic[8-10]. The temperature and heating rate during pyrolysis directly impact the degree of decomposition, cross-linking, and phase transformation in the precursor[11]. The cross-linking density and polymer structure, including functional groups and side chains, also influence the ceramic formation[12, 13]. Elemental composition, impurities, and post-treatment processes

such as annealing or sintering further modify the composition and properties of PDC ceramics. The atmosphere during pyrolysis is another important factor, with inert atmospheres like argon (Ar) and nitrogen (N_2) commonly used to prevent oxidation, while reactive atmospheres like hydrogen (H_2), ammonia (NH_3), water vapor (H_2O), or carbon dioxide (CO_2) can introduce chemical reactions and alter the composition[14-17].

In recent decades, several silicon-based PDCs have been synthesized and investigated for various applications[18-20]. These include materials like silicon carbide (SiC)[21, 22], silicon oxycarbide (SiCO)[23, 24], and silicon carbonitride (SiCN)[24]. SiC, for example, is known for its high-temperature stability and excellent mechanical properties, making it suitable for applications such as ceramic heaters. SiCO and SiCN, on the other hand, exhibit a combination of properties that make them attractive for use in corrosion-resistant coatings and micro-electro-mechanical systems (MEMS)[25-28].

This study focuses on the synthesis and characterization of silicon carbonitride (SiCN) ceramics. SiCN ceramics are produced using polycarbosilazanes as precursor materials. These polymers, when subjected to heat treatment at temperatures up to 1000°C, undergo a transformation into non-crystalline ceramics. This conversion process involves the elimination of organic components and the formation of a three-dimensional network of silicon, carbon, and nitrogen atoms[29, 30].

The resulting SiCN ceramics exhibit an amorphous matrix structure, meaning that they lack long-range order in their atomic arrangement. Instead of distinct crystalline regions, the ceramic material appears as a disordered network. Within this amorphous matrix, sp^2 carbon atoms, commonly referred to as free carbon (C_f), are embedded. The presence and morphology of free carbon have a significant influence on the properties exhibited by SiCN ceramics[31, 32].

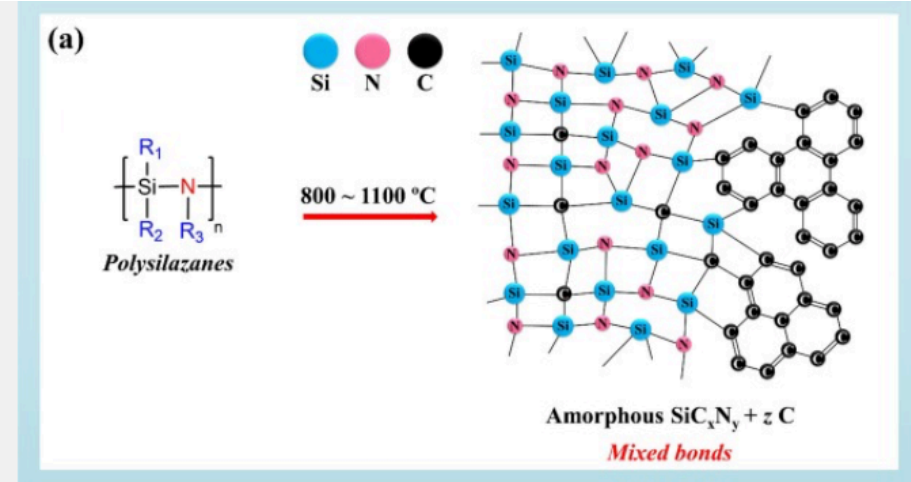

Figure 1.1: Amorphous SiCN ceramic chemical composition[31].

While the use of inert atmospheres like nitrogen is prevalent in synthesizing SiCN ceramics, a limited number of studies have explored the use of ammonia (NH_3) as a reactive atmosphere during pyrolysis. For instance, in 1999, Galusek et al. conducted experiments using NH_3 during the pyrolysis process and investigated its impact on the chemical composition of SiCN ceramics[33]. More recently, Sorarù et al. reported the synthesis of SiCN ceramics under NH_3 atmospheres[34].

Another system that has received significant attention is silicon oxycarbide (SiCO). Researchers have conducted numerous studies using reactive atmosphere pyrolysis (RAP) to explore the properties and applications of SiCO ceramics. For example, Narisawa et al. conducted a study in 2015 to investigate the effect of different atmospheres (H_2, CO_2, and Ar) on phase development in small SiCO spheres[35]. They also reported the synthesis of white SiCO ceramic powders and fibers using H_2 atmospheres[36]. Additionally, Sorarù et al. successfully synthesized transparent SiCO aerogels via a sol-gel process[37]. In this particular work, we employed a commercially available liquid polymer precursor called Ceraset Polysilazane 20 (PSZ20). This polymer has been extensively studied in previous research, and various pyrolysis results under inert atmospheres, particularly nitrogen, can be found in the literature. For instance, Markel et al. conducted theoretical calculations to study the crystallization of thermodynamically stable phases and high-temperature phase transformations in PSZ20 under inert

atmospheres[37]. They reported that SiCN ceramics synthesized from PSZ20 remain stable up to 1484°C, beyond which Si3N4 begins to crystallize into SiC.

The main objective of this current work is to investigate and compare the impact of hydrogen and nitrogen atmospheres on the thermal conversion of the Durazane1800 (another brand name for PSZ20) polymer into SiCN ceramics. We will study the chemical differences resulting from the different atmospheres by conducting analysis of the resulting ceramics using techniques such as IR spectroscopy, X-ray diffraction (XRD), Raman spectroscopy, and thermogravimetric analysis (TGA). This comprehensive characterization will provide valuable insights into the structural and compositional properties of the SiCN ceramics and enable a better understanding of the influence of atmospheric conditions on their formation.

Experimental Procedure

The experiment involves the synthesis and characterization of crosslinked polysilazane precursor Durazane1800, followed by pyrolysis at different temperatures and in different atmospheres. The resulting products were labeled NX or HX, where N represents nitrogen atmosphere, H represents hydrogen atmosphere, and X represents the pyrolysis temperature.

The synthesis process involved mixing Durazane1800 with 1.5% dicumyl peroxide (DCPO) using a magnetic stirrer until complete dissolution of DCPO occurred. The mixture was then placed in an oven at 150 °C for 1 hour to allow for crosslinking resulting in the formation of a transparent solid.

The pyrolysis of the crosslinked material was performed in two steps. First, the temperature was raised from room temperature to 400 °C, holding it for 1 hour. Then, the temperature was further increased to the desired pyrolysis temperature (ranging from 400 to 1000 °C) and held at that temperature for 1 hour. A heating rate of 2 °C/min and a gas flow rate of 500 ml/min were maintained throughout the pyrolysis process.

These products were subsequently analyzed using various characterization techniques to investigate the influence of the pyrolysis atmosphere on their properties.

Results:

Changing the pyrolysis temperature and atmosphere has an impact on the visual properties of the resultant material, specifically its color and transparency. At higher pyrolysis temperatures, the color of the material became darker. When the pyrolysis was carried out in a hydrogen atmosphere, the color of the material gradually changed with increasing temperature. It started as a pale yellow and progressed to orange, then brown, and finally black. Interestingly, even at higher temperatures, the material retained its translucent character in the hydrogen atmosphere until approximately 800°C. In contrast, when the pyrolysis was conducted in a nitrogen atmosphere, the resultant ceramics were already black and opaque at a lower temperature of 700°C. This indicates that the presence of hydrogen affects the chemical reactions and carbon structure formation differently compared to nitrogen. The resulting material in a hydrogen atmosphere seems to have a different composition or structure, leading to a non-black translucent material.

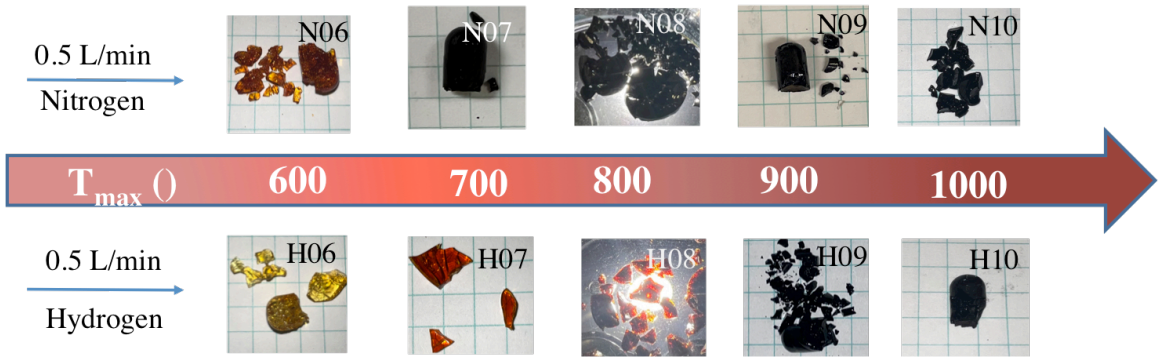

Figure 1.2: Photographs of Durazane1800-DCPO polymer pyrolyzed under different atmosphere.

During the pyrolysis, the precursor polymer undergoes thermal decomposition and various chemical reactions. The carbon content in the precursor polymer can be converted into amorphous carbon or carbon-rich phases. The presence of these carbon-rich structures or compounds in the SiCN ceramics can contribute to the darkening of their color, resulting in a black appearance. Hydrogen

as a reactive atmosphere during pyrolysis can influence the formation of amorphous carbon or free carbon through decarbonization process. These observations, removal of higher carbon through decarbonization, were also supported by the mass loss data. As the pyrolysis temperature was increased, a higher mass loss was observed until reaching 800°C. Beyond this point, the mass loss remained stable up to 1000°C in both nitrogen and hydrogen atmospheres. However, it is noteworthy that consistently higher mass loss was observed in the hydrogen atmosphere compared to the nitrogen atmosphere at all temperatures. For example, at 1000°C, a mass loss of 26% was recorded under the nitrogen atmosphere, whereas a higher mass loss of 33% was observed under the hydrogen atmosphere. To corroborate these observations further analyses were done on pyrolyzed materials. The results are discussed below.

Pyrolysis T (°C)	N_2	H_2
600	18	21
700	23	32
800	26	36
900	24	33
1000	26	33

Table 1.1: Mass loss recorded after the pyrolysis at different temperatures under N_2 or H_2

IR Analysis:

Infrared (IR) analysis was carried out on N_2 and H_2 – pyrolyzed samples. Analysis was done on Bruker ALPHA II compact spectrometer. The purpose of this analysis was to investigate the presence of functional groups in the samples. However, upon subjecting the samples to pyrolysis at temperatures above 700°C, all the peaks assigned to functional groups disappeared.

Interestingly, when the H_2-pyrolyzed samples were examined within the range of 700 - 900 cm^{-1}, four distinct peaks were observed. These peaks indicated the presence of certain functional groups or molecular vibrations. On the other hand, in the N_2-pyrolyzed samples, these peaks were not as clearly visible or pronounced.

This observation suggests that the pyrolysis process under a hydrogen atmosphere (H_2) retains carbon in sp^3 like configuration. However, the same effect was not as pronounced in the samples subjected to pyrolysis under a nitrogen atmosphere (N_2). To learn more about the Carbon present in sample, Raman analysis was performed as well. The results from Raman analysis are discussed below.

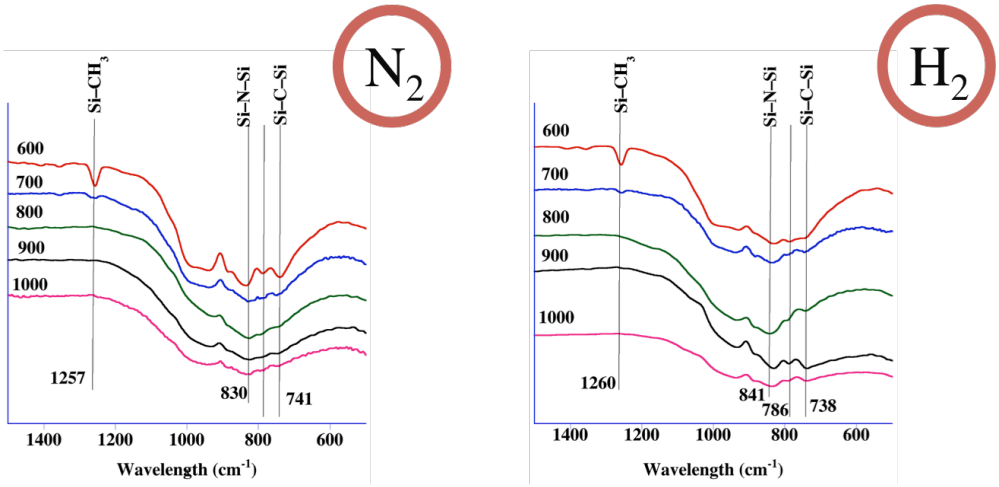

Figure 1.3: FT-IR spectra of i) samples pyrolyzed in N_2-atmosphere (left) and ii) samples pyrolyzed under H_2-atmosphere (Right)

Raman Analysis

Raman analysis was conducted using a Thermo Scientific DXR3 Raman microscope with a 532 nm laser wavelength and a 50x working distance. From the Raman spectra, two distinct signals were observed at wavenumbers of 1330 cm^{-1} and 1575 cm^{-1} in the sample that underwent pyrolysis under a hydrogen atmosphere. These peaks indicate the D and G bands, respectively. These bands are commonly observed in carbonaceous materials and play a significant role in the characterization of the carbon phase[31, 38-40]. The D band arises from disorder-induced vibrations in graphene layers, while the G band results from in-plane bond stretching of sp2-hybridized carbon atoms[40]. The presence and relative intensities of these bands provide insights into the degree of disorder and the graphitic structure of the carbonaceous material.

However, in contrast, the sample subjected to pyrolysis under a nitrogen atmosphere did not exhibit these peaks. Instead, a flat line was observed in the Raman spectrum, suggesting the absence or minimal presence of the corresponding molecular vibrations or functional groups in the nitrogen-pyrolyzed sample.

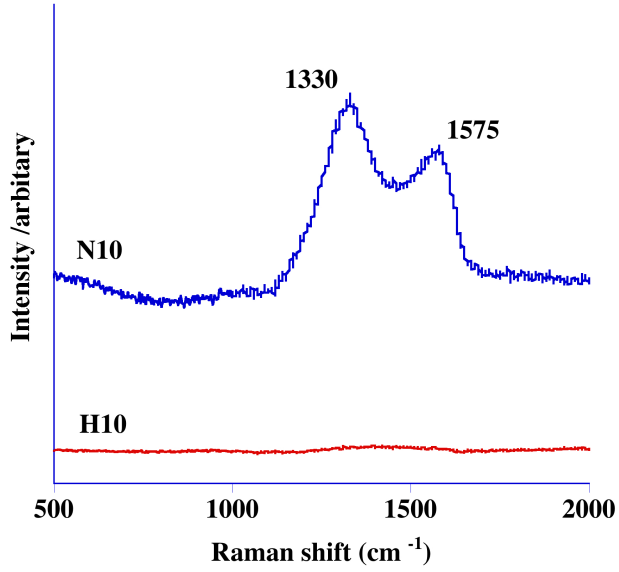

Figure 1.4: Raman spectra of sample pyrolyzed in N_2-atmosphere (blue) and sample pyrolyzed under H_2-atmosphere (red)

Chemical Composition

In order to investigate the impact of hydrogen as a reactive pyrolysis atmosphere on the resulting SiCN ceramic, particularly with regard to carbon content, chemical composition analysis was conducted on the samples.

	Si	C	N	O
H10	1	0.59±0.01	0.243± 0.004	0.86±0.03
N10	1	1.070±0.003	0.2428±0.0006	0.850±0.005

Table 1.2: Chemical compositions of samples H10 and N10

The results indicate a significant reduction in carbon content in sample H10 compared to N10. However, it is important to note that both samples exhibit high oxygen contents. The presence of oxygen in the final products poses challenges in determining whether the lower carbon content is a direct result of the hydrogen atmosphere or is influenced by the oxygen present during pyrolysis. The elevated oxygen content could be attributed to various factors, such as furnace leakage or the introduction of oxygen during the handling of the Durazane 1800 precursor.

To support this data and to confirm presence of oxygen EDX analysis were perform on the same sample. EDX result also showed the presence of oxygen. Even though the results doesn't match quantitatively but the ratio of oxygen to nitrogen is similar from chemical analysis and EDX results. To see if this impurity was just in that one sample or we really have higher contents of oxygen in SICN produced with method, another sample was produced the same way. And the EDX performed on this new sample also showed same ratios of oxygen to nitrogen.

Elements	Weight %			
	N10		H10	
	Old	New	Old	New
Si	15–23	13-20	18 - 33	14 - 30
C	34–42	47-59	13 - 28	37 - 59
N	6–8	15-16	5 - 8	12 - 21
O	35-37	9-19	47 - 50	14 - 27

Table 1.3: EDX analysis of old and new H10 and N10 samples

Further experiments, including using a new batch of polymer or modifying the furnace setup, are necessary to conclusively determine the effect of hydrogen atmosphere mainly on the carbon content.

Thermo Gravimetric Analysis

The thermal stability of amorphous SiCN samples, namely N10 and H10, was analyzed using a Thermogravimetric Analyzer (TGA) instrument. SDT 650 TA Instrument's analyzer was used for the analysis. Previously pyrolyzed samples of N10 and H10 were subjected to separate runs under a nitrogen (N_2) atmosphere, and the analysis was conducted up to a temperature of 1300°C. Each experiment began by equilibrating the instrument at 50°C for 20 minutes. Subsequently, the temperature was increased at a heating rate of 10°C per minute until it reached 800°C. From there, the heating rate was reduced to 5°C per minute, and the temperature was further increased until it reached 1300°C. The TGA curves obtained from these experiments are depicted in the graph below.

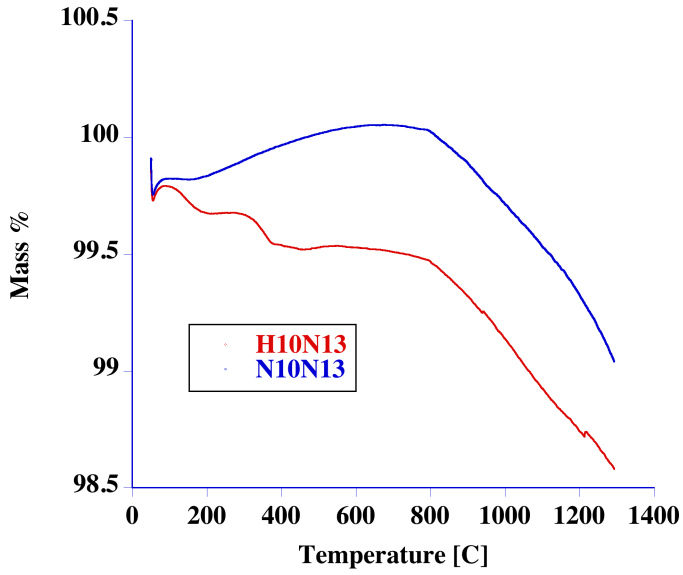

Figure 1.5: TGA spectra of samples pyrolyzed in N_2-atmosphere (blue) and sample pyrolyzed under H_2-atmosphere (red) taken again under N_2

The results revealed that both samples exhibited exceptional stability even at elevated temperatures. In the case of the N10 sample, the TGA analysis demonstrated that it experienced only a minimal mass loss of approximately 1% throughout the entire temperature range up to 1300°C. This indicates that the N10 sample can withstand high temperatures without undergoing significant decomposition or degradation. The high thermal stability of the N10 sample makes it a promising material for applications that require resistance to extreme temperatures.

Similarly, the H10 sample also exhibited excellent thermal stability, although slightly lower than that of the N10 sample. The TGA analysis showed that the H10 sample experienced a mass loss of approximately 1.5% up to 1300°C. While this is marginally higher than the mass loss observed in the N10 sample, it still indicates a high degree of stability, especially considering the significant temperature range.

However, it is important to note that additional experiments should be conducted to ensure the reproducibility of these findings. Two factors require further investigation: the mass gain observed in the N10N13 sample and the steps observed in the TG curve of the H10N13 sample around the temperature range of 300-400°C.

These unexpected observations may indicate variations in the sample preparation or potential impurities, which could affect the thermal stability analysis.

Thermal stability testing was conducted through furnace experiments on the N10 and H10 samples. In these experiments, the samples were subjected to a second pyrolysis process under an N_2 gas atmosphere. The pyrolysis was carried out at 800°C with a heating rate of 2°C per minute, and a hold at the peak temperature (Tp) was applied. Remarkably, both samples exhibited negligible mass losses during this second pyrolysis under N_2. To ensure reproducibility, the experiments were repeated, and consistent mass losses were observed in both instances. These findings align with the results obtained from the TGA experiments, confirming the high thermal stability of these materials even at elevated temperatures.

Samples	Empty boat	Boat + sample	After pyrolysis	% mass loss
H10_N08	56.2811	56.8038	56.8028	0.19
N10_N08	55.5058	55.8700	55.8673	0.74

Table 1.4: Mass loss recorded after the repyrolysis of N10 and H10 at 800 °C

Raman analysis was performed on the repyrolyzed samples of N10 and H10 to investigate the effect of temperature on the carbon or free carbon present in these materials. Surprisingly, similar Raman spectra were observed for both N10 and H10 samples after the repyrolysis process. This indicates that the temperature treatment during repyrolysis did not significantly affect the carbon structure or the presence of free carbon in either material. The consistent Raman spectra suggest that the thermal stability of the carbon components in N10 and H10 remains intact even after undergoing the second pyrolysis process.

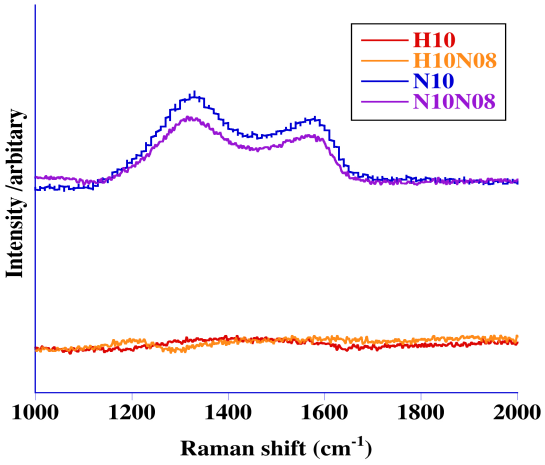

Figure 1.6: Raman analysis of repyrolyzed samples N10 and H10 at 800 °C

X-Ray Diffraction Analysis:

X-Ray Diffraction (XRD) analysis was carried out on D8 instrument from Bruker with CuKa (1.54 Å) radiation, to verify the amorphous nature of the ceramics obtained from the pyrolysis of N10 and H10 samples at 1000°C. For this The XRD patterns obtained for both N10 and H10 exhibited broad humps rather than sharp peaks, indicating the absence of long-range crystalline order. This confirms that both materials remain in an amorphous state even after the pyrolysis process. Similar results have been observed in other studies investigating the pyrolysis of SiCN materials at 1000°C. These findings further support the understanding that the pyrolysis process at this temperature retains the amorphous nature of SiCN ceramics.

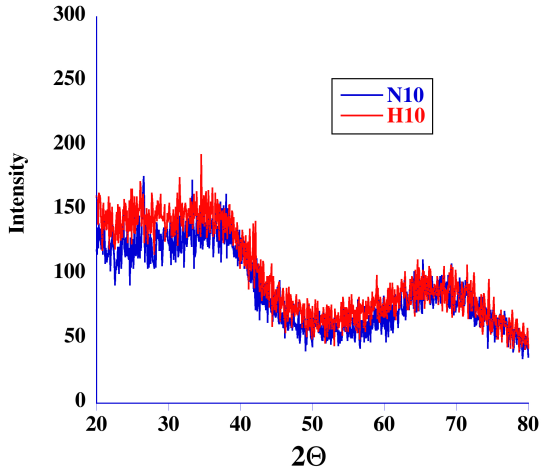

Figure 1.7: XRD analysis of samples N10 and H10

Summary

The utilization of hydrogen (H_2) as a reactive atmosphere during the pyrolysis of polysilazane has several notable effects on the resulting silicon carbonitride (SiCN) ceramics. Firstly, it influences the color of the amorphous SiCN ceramics, providing a distinct visual difference. Moreover, even at high temperatures such as 800 °C, the H2 atmosphere helps maintain the translucency of the ceramics, preserving their optical properties.

In terms of chemical composition, the presence of H_2 during pyrolysis plays a crucial role. Infrared (IR) analysis reveals that the H_2 atmosphere promotes the retention of carbon in an aliphatic (sp3-like) configuration within the SiCN ceramics. This suggests that carbon atoms are bonded to other non-carbon atoms, such as nitrogen and silicon, in a more linear or branched fashion, enhancing the aliphatic character of the material.

Raman spectroscopy analysis further demonstrates the impact of the H_2 atmosphere. It shows that the use of H_2 prevents the formation of extended carbon segregations within the SiCN ceramics. This is significant as extended carbon segregations can lead to the development of graphitic structures or the clustering of carbon atoms, potentially altering the properties of the material. By hindering such carbon clustering or graphitization, the H_2 atmosphere helps maintain the amorphous nature of the SiCN ceramics.

Additionally, the pyrolysis of polysilazane in an H_2 atmosphere results in higher mass loss compared to other atmospheres. This indicates that the H_2 environment promotes the elimination of more carbon containing species such as methane CH_4 during the pyrolysis process

Lastly, thermogravimetric analysis (TGA) confirms that SiCN ceramics produced under not just inert but also H_2 atmosphere exhibit thermal stability at least up to 800 °C. This demonstrates the effectiveness of the H_2 atmosphere in preserving the structural integrity of the ceramics at elevated temperatures, making them suitable for high-temperature applications.

In summary, the use of hydrogen as a reactive atmosphere during the pyrolysis of polysilazane has multiple effects on the resulting SiCN ceramics. It impacts the color and translucency, retains carbon in an aliphatic configuration, prevents the formation of extended carbon segregations, leads to higher mass loss, and produces thermally stable ceramics. . However, it is important to consider the presence of a high amount of oxygen in the ceramic composition. The elevated oxygen content raises questions about whether the observed differences between inert and reactive atmosphere is solely attributed to the H_2 atmosphere or if the oxygen atmosphere also contributes to these effects.

Future work

1. **Chemical composition:** As discussed earlier the chemical composition is still a nagging question and need to be resolved. To address this ambiguity and elucidate the effect of hydrogen as pyrolysis atmosphere on the chemical compostion, further experiments are necessary. These experiments could involve using a new batch of polymer or modifying the furnace setup to ensure an atmosphere free from potential oxygen contamination. By conducting additional studies under controlled conditions, it will be possible to conclusively determine whether the higher mass loss and lower carbon content in the chemical composition is indeed a result of the hydrogen atmosphere or if oxygen-related factors play a significant role in this phenomenon.
2. **Phase stability of carbon:** Phase studies were conducted on PSZ20-DCPO samples using a slightly different synthesis method, but the results are still noteworthy. The synthesis process involved cross-linking Durazane 1800 with DCPO at 250°C for 4 hours, followed by ball milling to obtain homogeneous powders. Subsequently, pyrolysis was carried out under either nitrogen or hydrogen atmosphere at 1000°C. The resulting samples were then annealed under argon for 5 hours at various annealing temperatures. Raman analysis was performed on the annealed samples.

   The Raman analysis revealed interesting findings. For the samples pyrolyzed at 1000°C, those under nitrogen atmosphere exhibited signals attributed to the D and G peaks, indicating the presence of carbon-based structures. However, similar signals were not observed in the samples pyrolyzed under the hydrogen atmosphere. Instead, a flat line was observed, suggesting a lack of distinct carbon-related peaks. This indicates that the formation of extended carbon segregations may be suppressed in the hydrogen-pyrolyzed samples at this temperature.

   On the other hand, for the samples pyrolyzed at 1300°C, strong D and G peaks were observed even in the hydrogen-pyrolyzed samples. This suggests that at this higher temperature, extended carbon segregations are formed even in the hydrogen-pyrolyzed samples. Further analysis is needed to determine the specific temperature range at which these carbon segregations start to form in the

hydrogen-pyrolyzed materials. This information is crucial for understanding the thermal stability of the amorphous carbon phase in hydrogen-pyrolyzed samples and how it evolves with increasing temperatures.

In summary, the phase studies conducted on the PSZ20-DCPO samples showed intriguing results. The Raman analysis indicated the presence of carbon-based structures in the nitrogen-pyrolyzed samples at 1000°C, while the hydrogen-pyrolyzed samples exhibited a lack of distinct carbon-related peaks. However, at 1300°C, extended carbon segregations were observed in the hydrogen-pyrolyzed samples. Further investigation is necessary to determine the temperature range for the formation of carbon segregations in hydrogen-pyrolyzed materials and the stability of the amorphous carbon phase.

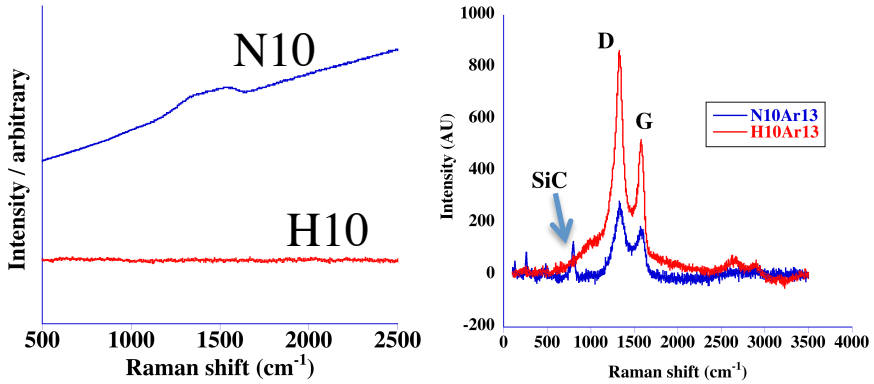

Figure 1.7: Raman analysis of samples N10 and H10 (left) and samples H10Ar13 and N10Ar13 (right)

3. **Phase development:** Phase development studies were conducted on materials annealed at 1500°C for 5 hours, namely H10Ar15 and N10Ar15. The X-ray diffraction (XRD) patterns of these samples exhibit significant differences in the number of peaks and their intensities. Further analysis was performed using Jade software to determine the phases present and their respective content in each sample.

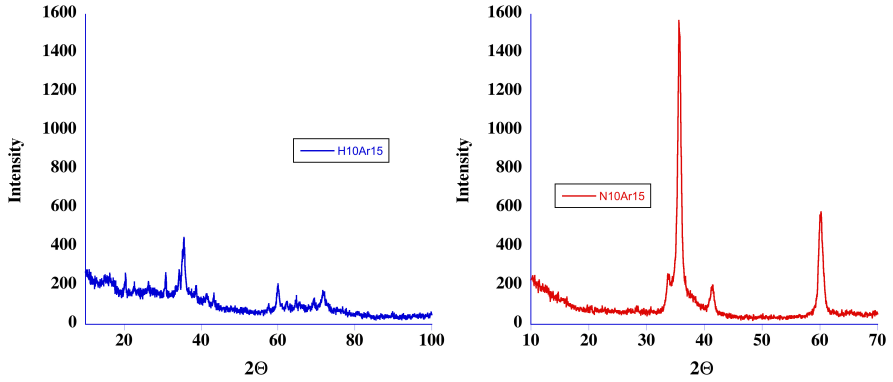

Figure 1.8: XRD analysis of samples H10Ar15(blue) and H10Ar15(red)

The refinement results indicate that in N10Ar15, only one phase, SiC, is present with a small amount of Si3N4. On the other hand, H10Ar15 still contains approximately one-third of its phase content as Si3N4, while the remaining two-thirds consists of SiC. These results are consistent with literature on the pyrolysis of PSZ20 at 1500°C under an argon atmosphere. According to the theoretical calculations conducted by Markel et al., SiCN ceramics synthesized using PSZ20 are in a three-phase region, namely Si3N4+SiC+Cfree, up to a temperature of 1484°C under argon. Above 1484°C, the free carbon (Cfree) reacts with Si3N4 to form SiC, releasing N2 as a byproduct, which has been experimentally confirmed using mass spectrometry.

Furthermore, it has been reported that the crystallization of Si3N4 at a pyrolysis temperature of 1400°C leads to the formation of β-SiC. This is in line with the higher content of β-SiC (3C-SiC) observed in N10Ar15. The presence of a hump in the XRD pattern of H10 at 10-20 theta values supports the Raman results, indicating that the sample has not completely crystallized yet and the amorphous phase is still present.

To further investigate the phase development, the annealing time was extended from 5 hours to 48 hours to ensure the complete crystallization of the amorphous phase. Surprisingly, the XRD spectra of these samples yielded unexpected results. Both H10Ar15 (48) and N10Ar15 (48) showed the presence of Si3N4 and SiC phases in similar ratios. However, H10Ar15 (48) exhibited the additional presence of elemental Si, which was a highly intriguing observation.

The presence of elemental Si at such low temperatures raises questions about the mechanisms behind its evolution. Furthermore, it is interesting to note that the amount of Si3N4 is higher in N10Ar15 (48) compared to N10Ar15 (5). These findings suggest that the crystallization process is complex and not yet fully understood. To gain a deeper understanding of this crystallization process and the factors influencing the phase development, systematic studies are necessary.

Additional investigations are required to elucidate the underlying mechanisms responsible for the unexpected presence of elemental Si and the variations in Si3N4 amounts between different annealing conditions. These systematic studies would provide valuable insights into the crystallization behavior and phase transformations occurring at different annealing times and temperatures.

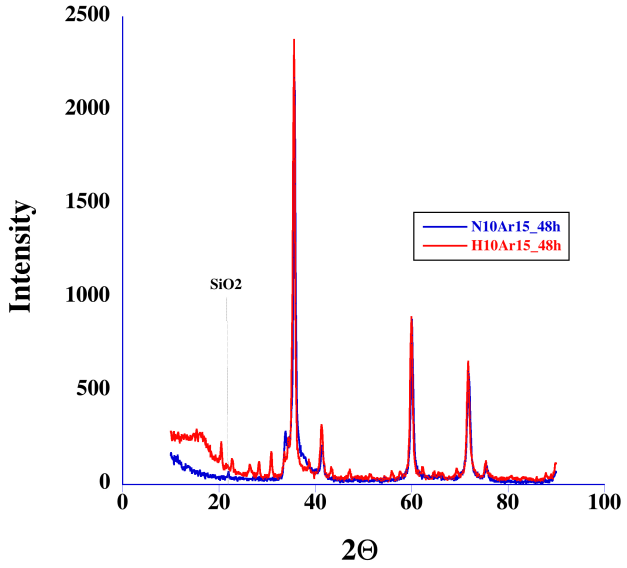

Figure 1.9: XRD analysis of samples H10Ar15 (blue) and H10Ar15 (red) annealed for longer time

In summary, the phase development studies conducted on the materials annealed at 1500°C revealed distinct differences between H10Ar15 and N10Ar15. The refinement results confirmed the presence of SiC and Si3N4 in N10Ar15, while H10Ar15 contained a higher proportion of Si3N4 along with SiC. However increasing the annealing time reveals some interesting results like evolution of elemental Si. Overall, these findings emphasize the complexity of the crystallization process and the importance of conducting systematic studies to unravel the underlying mechanisms. Further investigations are required to shed light on the evolution of elemental Si and the variations in Si3N4 content, providing valuable insights into the phase transformations and crystallization behavior at different annealing times and temperatures.

4. **Intrinsic Porosity:** We initially observed a significant increase in mass loss around 800°C in the Durazane1800_DCPO material. We hypothesized that this was due to the development of intrinsic porosity during pyrolysis, leading to the evolution of gases. However, after 800°C, these pores seemed to collapse, trapping some of the evolving species and resulting in a less pronounced difference in mass loss.

   To further investigate this hypothesis, additional pyrolysis experiments were conducted on the same material. These experiments involved introducing hold steps of 4 hours at different temperatures under hydrogen atmospheres. The temperature was raised from room temperature to the hold temperature (THold), where it remained constant for 4 hours, before further raising it to 1000°C, using a heating rate of 2°C/min. The mass loss was recorded for each experiment, and the results are presented in the table below.

   The table includes two datasets: one where the temperature in the first column represents the hold temperature (THold), with a constant pyrolysis temperature of 1000°C. The second dataset shows the pyrolysis temperature (Tp) at which the sample was held for 1 hour. From the data, we can observe that mass loss increases from 600°C to 800°C for both THold and Tp, and then decreases again at 900°C and 1000°C. Additionally, we noticed that the mass loss is higher for THold compared to Tp.

Temperature [°C]	Mass loss [%]	
	T_{Hold}	T_p
600	32 ± 2	21
700	35 ± 0.5	32
800	37 ± 1	36
900	–	33
1000	31.5 ± 0.5 (new data point)	33

Table 1.5: Mass loss after pyrolysis at 1000°C recorded under H_2 with hold at different temperatures and compared with previous mass loss data under H_2

These findings support our initial observations, but more in-depth investigations are required, particularly regarding porosity measurements. To gain more reliable data for this study, it is necessary to conduct studies using porous materials, rather than relying on bulk materials like the one used in this study. By focusing on porosity measurements and employing porous materials in our experiments, we can better understand the role of intrinsic porosity in the observed mass loss behavior during pyrolysis.

Chapter 2: Thermal Decomposition of Durazane 1800 under forming gas in comparison with Nitrogen

Introduction

Thermal gravimetric analysis coupled with mass spectroscopy (TG-MS) is a widely used and powerful technique employed for the quantitative and in-depth study of the decomposition behavior and polymer-to-ceramic conversion of materials[41]. Additionally, the effect of heating rates on the decomposition behavior can be studied to investigate kinetic parameters such as activation energy[42].

In a notable study conducted by Markel et al., they examined the TG-MS analysis results of two specific polymer precursors, PSZ10 and PSZ20. The decomposition behavior was analyzed under inert atmospheres to better understand the transformation processes[42].

The typical TG-MS of these SiCN shows a distinct three-stage decomposition process for the polymer precursors. In the first stage, which occurs at temperatures below 300 °C, the mass loss was attributed to the evaporation of small oligomers. These oligomers are formed due to crosslinking reactions at relatively low temperatures.

Moving into the second stage, the temperature range of 300 to 1000 °C, the polymer precursors undergoes pyrolysis. This leads to the formation of an amorphous network comprising silicon-carbon-nitrogen (Si-C-N). During this pyrolysis process, mass spectrometry detected the release of hydrogen and methane gases, indicating the generation of volatile components[42].

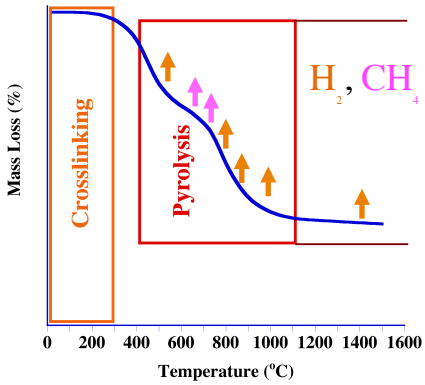

Figure 2.1: A typical TG curve for SiCN preceramic polymers

The third stage, observed at temperatures higher than 1000 °C, revealed intriguing behavior. Between 1000 and 1300 °C, the mass remained relatively constant. However, when the samples were pyrolyzed at even higher temperatures, such as 1400 and 1500 °C, there was a significant mass loss. Further analysis through mass spectrometry identified this mass loss as being associated with the release of nitrogen gas.

For the PSZ20-derived SiCN ceramics, the material is generally found to be composed of three amorphous phases: a-Si3N4, a-SiC, and a-C, up to temperatures of 1485 °C. Interestingly, beyond this temperature, i.e., above 1485 °C, a reaction occurs between a-Si3N4 and a-C through carbothermal reduction. This reaction results in the formation of α/β SiC[31, 42]. Overall, the TG-MS analysis allowed for a comprehensive understanding of the various stages of decomposition and transformation processes involved in the conversion of polymer precursors to SiCN ceramics. These insights are invaluable for material scientists and engineers working on advanced ceramics, as they provide crucial information for the optimization and design of ceramics with desired properties for various applications.

Current work focuses on studying the thermal decomposition of Durazane 1800 under forming gas (Mixture of 3% H2 and 97% N2) and comparing the results with decomposition under N2.

Experimental Procedure:

The synthesis process involved the cross-linking of Durazane 1800 with DCPO at a temperature of 250°C for a duration of 4 hours. After this initial step, ball milling was performed to achieve a homogeneous mixture of powders. These powders were then subjected to Thermal Gravimetric Analysis (TGA) under two different atmospheres: nitrogen (N_2) and forming gas. Throughout the analyses, all other parameters in the heating profile were kept constant, with the exception of the heating rates.

The heating profile used in the TGA experiments commenced by ramping up the temperature to 50°C and holding it there for 20 minutes to ensure that both the reference and sample pans reached thermal equilibrium. Following this equilibration step, the temperature was further ramped up to 1000°C, and various heating rates were applied during this ramping phase.

To distinguish between different TGA experiments, the samples were appropriately labeled. For instance, samples analyzed under nitrogen atmosphere were denoted as NX, where N stands for nitrogen, and X represents the heating rate values such as 02, 05, 10, 20, and 50°C/min. Similarly, samples analyzed under forming gas atmosphere were labeled as HX, with H representing forming gas ($3\%H_2 and 97\%N_2$), and again X signifying the specific heating rate used in the experiment.

The obtained TGA results are discussed below. They provide valuable insights into the thermal behavior of the synthesized powders under different conditions. The data allows the understanding of the weight changes in the samples as a function of temperature, providing essential information about the decomposition and transformation processes occurring in the material.

Results:

The Thermo gravimetric analysis (TGA) results revealed some interesting trends for the synthesized powders under both nitrogen and forming gas atmospheres, across all heating rates.

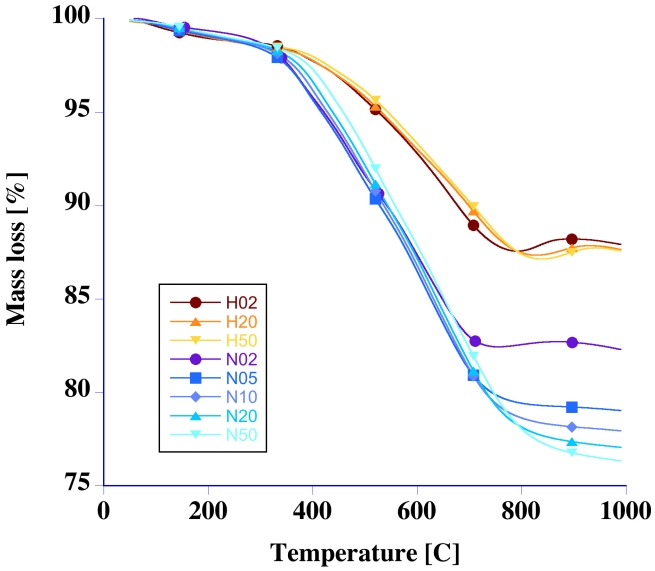

Figure 2.2: TG curves recorded for PSZ20-DCPO powders under N_2 and forming gas atmosphere with different heating rates.

As anticipated, the TGA curves indicated that the maximum weight loss occurred in a temperature range of approximately 350°C to 750°C. This region is critical because it corresponds to the decomposition of the precursor materials and the initiation of various chemical reactions leading to the formation of the desired product, in this case, SiCN ceramics.

However, the more intriguing observation was that the mass loss under forming gas atmosphere was consistently lower compared to the mass loss under nitrogen gas atmosphere, across all heating rates studied. This finding suggests that the presence of forming gas (a mixture of hydrogen and nitrogen) during the TGA experiments had a significant influence on the decomposition behavior of the synthesized powders.

The lower mass loss under forming gas indicates that the decomposition of the precursor materials and the subsequent transformations leading to SiCN

ceramics were less pronounced or occurred at higher temperatures compared to those under nitrogen atmosphere. This difference in mass loss can be attributed to the distinct gas environments of nitrogen and forming gas. Forming gas contains hydrogen, which is known for its reducing properties. The presence of hydrogen during the TGA experiments could have suppressed certain decomposition reactions or reduced the extent of oxidation processes, leading to a milder decomposition profile and lower weight loss[27]. On the other hand, nitrogen is an inert gas that does not actively participate in chemical reactions, which might have allowed for a more pronounced decomposition process and higher mass loss.

The variation in mass loss under different gas atmospheres can also be related to the thermodynamic stability of intermediates formed during the decomposition. Depending on the gas environment, certain intermediates may be more or less stable, impacting the overall decomposition behavior.

Indeed, the observations made from the TGA results are further corroborated by the Differential Thermogravimetry (DTG) curves. Under the nitrogen atmosphere, it was observed that as the heating rate was increased, the mass loss also increased. This finding indicates that the decomposition processes became more pronounced and occurred at higher temperatures when the heating rate was elevated.

Summary

In this study, thermal decomposition of PSZ20 preceramic polymer was studied under forming gas in comparison with N_2. TGA revealed interesting differences in the decomposition behavior of PSZ20 under different gases. The presence of forming gas influenced the decomposition behavior, resulting in lower mass loss compared to nitrogen. DTG supported these findings, showing milder decomposition under forming gas. Similar experiment performed in furnace resulted in somewhat similar mass loss trends, however not enough data to support TGA findings. Also, X-ray diffraction (XRD) analysis did not show significant differences in phase formations. Overall, the study highlights the importance of gas atmosphere and heating rates influencing the decomposition behavior and

properties of SiCN ceramics. Further investigations using complementary analytical techniques are necessary to gain a comprehensive understanding of the thermal decomposition of the precursor material under forming gas atmosphere. It is also important to investigate the the differences observed in forming gas are indeed the result of high partial pressure of H_2 and not the possible oxygen impurity. Overall more investigations are needed to conclude the results.

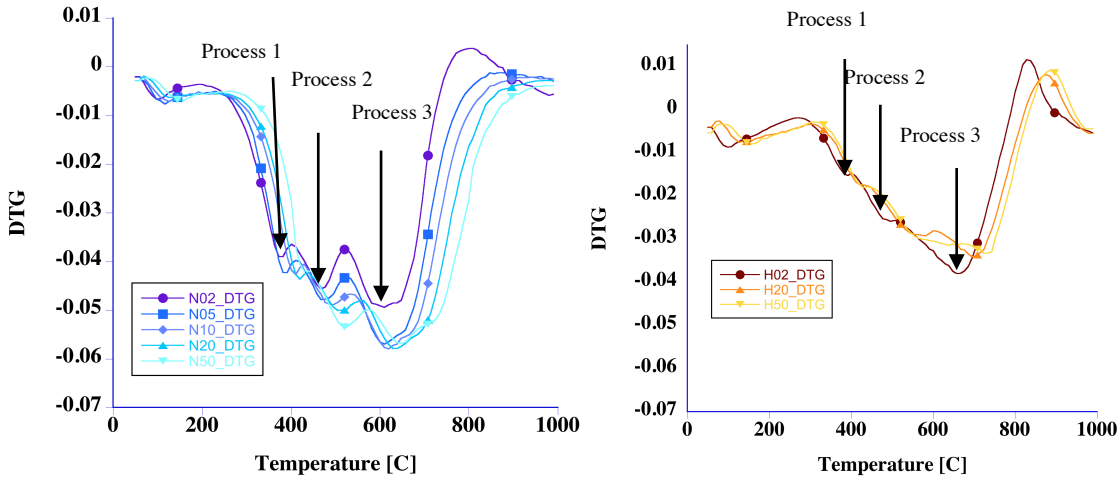

Figure 2.3: Differential Termogravimetric (DTG) curves of PSZ20-DCPO powder samples under N_2 and forming gas atmosphere with different heating rates.

Analyzing the DTG curves, it became evident that there were three distinct processes occurring during the decomposition of the synthesized powders. These processes correspond to different stages of decomposition, which are typically characterized by weight loss peaks in the DTG curves. Notably, with an increase in heating rate, the temperature at which each process occurred shifted to higher values. This shift indicates that the decomposition reactions were kinetically influenced, and the higher heating rates accelerated the reactions, causing them to take place at higher temperatures.

On the other hand, under the forming gas atmosphere, similar to nitrogen, the DTG curves also revealed the presence of three processes during the decomposition of the powders. However, these processes were not as pronounced as observed in the nitrogen atmosphere. The peaks in the DTG curves were less

sharp, suggesting that the decomposition was milder and more gradual under forming gas conditions.

Furthermore, the shift in the temperature at which these processes occurred under forming gas was not as prominent as in the case of nitrogen. This observation indicates that the presence of forming gas, particularly hydrogen, had a stabilizing effect on the decomposition reactions. Hydrogen's reducing properties likely suppressed some of the decomposition pathways or hindered oxidation processes, leading to a smoother and less distinct decomposition behavior.

Overall, the DTG curves provided additional insights into the decomposition processes and their temperature dependence under different gas atmospheres and heating rates. The DTG analysis supported the initial findings from the TGA experiments, confirming that forming gas had a mitigating effect on the decomposition of the synthesized powders compared to nitrogen. These combined results offer valuable guidance for optimizing the synthesis process and understanding the role of gas environments in tailoring the properties of SiCN ceramics for specific applications.

In continuation of the investigation, additional experiments were conducted using a furnace setup to further explore the synthesis and properties of the materials. The first step in the synthesis process involved the crosslinking of Durazane 1800 at 250°C for a duration of 4 hours. After the crosslinking process, the resulting material was subjected to ball milling to ensure a homogeneous powder mixture.

Subsequently, the homogeneous powder obtained from the ball milling was pyrolyzed at 1000°C under a forming gas atmosphere, and this pyrolysis step was performed using various heating rates. The mass loss during the pyrolysis process was recorded for all the runs. To ensure accuracy and assess the consistency of the results, some of the runs were repeated multiple times to obtain the deviations in mass loss.

In order to investigate the effects of further heat treatment, selected samples were subsequently annealed at 1500°C. The annealing process was carried out under an argon atmosphere with a constant heating rate of 10°C per minute. The

mass loss data was again recorded for these annealed samples to understand any additional changes that occurred during this heat treatment step.

Heating rate °C/min	Mass loss (%)		
	Pyrolysis		Annealing (Run 1)
	Run 1	Run 2	
2	12	19	11
5	18	–	39
10	17	18	38
20	16	–	27
50	6	4	20

Table 2.1: Mass loss data of pyrolysis of PSZ20-DCPO powders at 1000°C with different heating rates under Forming gas atmosphere.

During the experimental investigation, the mass loss data obtained did not exhibit a clear and distinctive trend. Across all heating rates used during the pyrolysis step under forming gas atmosphere, the mass loss showed relatively similar values, with all results falling within a 3% deviation from the average of approximately 15% mass loss. This lack of significant variation in mass loss among different heating rates suggested that the pyrolysis process was relatively robust and not highly sensitive to changes in the heating rate within the tested range.

However, one noteworthy observation was made for the sample subjected to the highest heating rate of 50°C per minute. In this case, the mass loss recorded during the pyrolysis step was notably lower compared to the other heating rates. This result indicated that the extremely rapid heating rate of 50°C per minute might have influenced the decomposition kinetics, leading to a less pronounced mass loss during pyrolysis.

Interestingly, during the subsequent annealing step conducted under an argon atmosphere at a constant heating rate of 10°C per minute, the mass loss data

showed a different trend. The annealing process resulted in a higher mass loss compared to the pyrolysis step, regardless of the heating rate used during pyrolysis. This increase in mass loss during annealing suggested the occurrence of additional decomposition or transformation processes, which might be associated with the crystallization of certain phases or other structural changes in the material.

The absence of a clear trend in mass loss during pyrolysis, except for the high heating rate case, indicated that the pyrolysis step was relatively insensitive to minor variations in the heating conditions within the tested range. On the other hand, the notable increase in mass loss during annealing highlighted the importance of the post-pyrolysis treatment in influencing the final composition and properties of the SiCN ceramics.

The lack of a distinct trend in mass loss during pyrolysis and the contrasting results observed during annealing underscored the complexity of the material's thermal behavior and its sensitivity to specific heat treatment conditions. These findings suggested that achieving precise control over the synthesis process and obtaining desired material properties may require careful optimization of the annealing step after pyrolysis.

Overall, the mass loss data provided valuable insights into the thermal stability and transformation processes of the synthesized powders under different heat treatment conditions. While the pyrolysis step showed consistent mass loss across various heating rates, annealing resulted in higher mass loss, indicating the occurrence of additional changes in the material. These observations offer valuable directions for further investigation and fine-tuning of the synthesis process to achieve the desired characteristics in SiCN ceramics for potential applications.

The mass loss data did not show any define trend. Within the 3 % limit of average of 15 % mass loss all heating rates resulted in similar mass loss except for the 50 C/min which resulted in very low mass loss. Annealing resulted in higher mass loss than compared to pyrolysis step. Visual observations as well support the mass loss data.

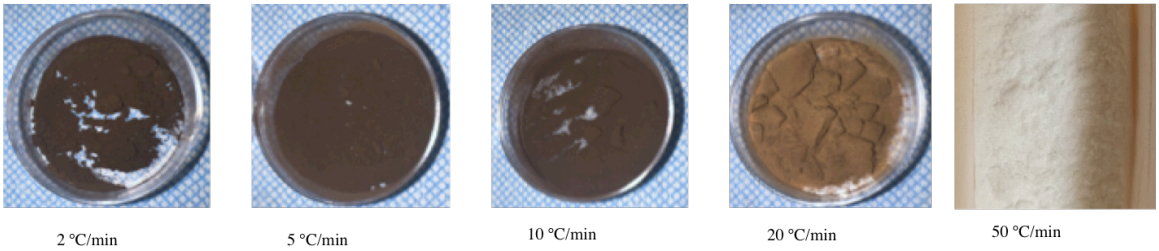

Figure 2.3: Photographs of pyrolyzed samples of PSZ20-DCPO powders at 1000°C with different heating rates under Forming gas atmosphere.

During the experimental analysis, the pyrolyzed materials obtained from different heating rates showed minimal visual differences, except for the sample pyrolyzed at the highest heating rate of 50°C per minute. For the majority of the samples, the appearance and color remained relatively consistent across various heating rates, indicating a similar level of decomposition and transformation during the pyrolysis process.

However, the sample pyrolyzed at 50°C/min exhibited a distinct characteristic. It showed minimal mass loss compared to the other samples, and its color did not undergo any noticeable change. This observation indicated that the extremely rapid heating rate of 50°C per minute might have suppressed the extent of decomposition and hindered the occurrence of significant transformations in the material.

The lack of substantial visual differences among the pyrolyzed materials, except for the high heating rate case, further supported the notion that the pyrolysis process was relatively insensitive to minor variations in the heating conditions within the tested range. It also suggested that the other heating rates used during pyrolysis were not drastic enough to cause prominent changes in the appearance or color of the resulting materials.

These visual observations, in conjunction with the mass loss data, provide valuable insights into the impact of heating rates on the pyrolysis process and the resulting material properties. The finding that the majority of the samples exhibited similar appearances and colors despite varying heating rates suggested that the

decomposition and transformation reactions were quite consistent within the tested range.

Following the annealing step, the annealed samples were subjected to X-ray diffraction (XRD) analysis to gain deeper insights into the phase formation and understand the influence of forming gas and heating kinetics on the resulting crystalline phases in the SiCN ceramics.

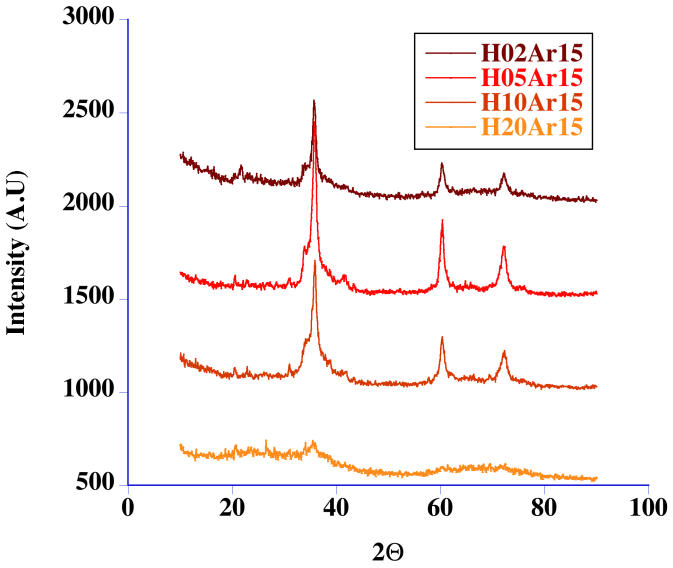

Figure 2.4: XRD analysis Forming gas pyrolyzed samples pyrolyzed with different heating rates up to 1000°C and then annealed at 1500°C under Ar

The XRD analysis of the samples pyrolyzed under forming gas at different heating rates did not reveal any notable observation. Up to a heating rate of 10°C per minute, there were no significant differences observed in the XRD patterns of the samples. The diffraction patterns were quite similar, indicating similar crystallographic structures and phase formations for these samples.

The samples pyrolyzed using higher heating rates of 20°C and 50°C/min did not exhibit clear peaks corresponding to crystalline phases. Instead, they produced broad humps in the XRD patterns, indicating the absence of well-defined crystal structures. The presence of broad humps in the XRD patterns suggests that the samples pyrolyzed at higher heating rates did not crystallize effectively during the heat treatment. The rapid heating at 20°C and 50°C per minute might have affected

the kinetics of phase formation, hindering the development of well-defined crystallographic structures. As a result, the samples pyrolyzed at these higher rates retained their amorphous or disordered nature.

Despite conducting the furnace experiment and subsequent XRD analysis, the results did not provide substantial evidence to support the observations seen in the TGA studies regarding the mass loss trends. The TGA experiments had indicated that the mass loss was influenced by various factors such as forming gas atmosphere, heating rates, and the annealing step. However, the XRD analysis of the annealed samples did not reveal any strong correlation with the observed mass loss trends.

As a result, additional complementary analytical techniques and further investigations might be necessary to gain a comprehensive understanding of the thermal decomposition of durazane1800 under forming gas atmosphere.

Chapter 3: Transparent SiCN material

Introduction:

When transitioning from "transparent" polymers that contain aliphatic carbon side groups to black ceramics, a notable transformation occurs characterized by the agglomeration of excess carbon into extended aromatic units and graphite-like structures[32]. This change in material properties is attributed to the presence of so-called sp2-like carbon, which is responsible for the black appearance[43].

To preserve the transparency of the material, it is essential to prevent the formation of sp2-like carbon structures. This can be achieved through a two-fold approach. One approach is promoting the retention of sp3-like carbon. By encouraging the carbon atoms to maintain sp3 hybridization, they remain bonded in a tetrahedral arrangement, which typically results in transparent materials. Controlling the pyrolysis process conditions and optimizing the reactive gas atmosphere can achieve this. And another way is eliminating "excess" carbon directly (decarbonization)[31, 36, 44]: The excess carbon that leads to the formation of sp2-like structures can be removed from the material. One effective method for achieving this is by using hydrogen gas (H2) as a reactive gas during the pyrolysis process. Hydrogen has a strong reactivity with carbon, and it acts as a reducing agent, combining with excess carbon to form volatile hydrocarbons, which can escape the material as gas[42]. This process, known as decarbonization, helps in maintaining the sp3-like carbon arrangement and thereby preserving transparency[37].

By employing a pyrolysis process that incorporates hydrogen gas as a reactive agent, the formation of sp2-like carbon can be effectively suppressed, ensuring that the material retains its transparency[44]. Moreover, this approach offers the added advantage of removing excess carbon from the material, leading to improve optical properties and preventing the development of black ceramics.

In the pyrolysis process of bulk SiCN (Durazane1800-DCPO) materials conducted under a hydrogen atmosphere, it was observed that the translucent character of the material was retained. Building on this observation, a new

hypothesis was formulated, suggesting that the use of porous materials would further enhance the evolution of carbon under a hydrogen atmosphere. The rationale behind this hypothesis is that the presence of pores in the material would reduce the diffusion path for carbon evolution during the pyrolysis process. As a result, the synthesis of porous materials was undertaken to test this hypothesis. Two different cross linkers, divinylbenzene (DVB) or Tetravinylsilane (TVS), were used for the synthesis to produce starting materials with different carbon content to start with. Below, we provide a detailed description of the synthesis method employed for the porous materials.

Experimental Procedure:

Two different precursors were used for the synthesis. Briefly, polymeric aerogels (**pa**) were prepared by crosslinking polymethylvinylsilazane (Ceraset PSZ20: Merck KGaA) with divinylbenzene (DVB), or Tetravinylsilane (TVS) in 1:2 mass ratios. Crosslinking is carried out in 85-volume % of cyclohexane in presence of 10 µL of Karstedt's catalyst in Parr vessels at 150°C for 6 h. Once the wet gel was produced, it was washed using solvent for 10 times to remove unreacted materials. Next it was dried using super critical dryer[7].

Figure 3.1: Chemical structure of divinylbenzene (DVB) (left) and Tetravinylsilane (TVS) (right)

Results:

After successfully producing preceramic aerogels, we conducted pyrolysis experiments under hydrogen or nitrogen atmospheres at different temperatures. The pyrolysis process followed the usual heating profile as in previous attempts. The resulting ceramic aerogels, namely PSZ20-DVB and PSZ20-TVS, showed little

visual difference between them. However, both ceramic aerogels failed to achieve transparency due to the presence of a significant amount of carbon introduced by the crosslinkers. It became evident that starting with a high carbon content was not a favorable approach.

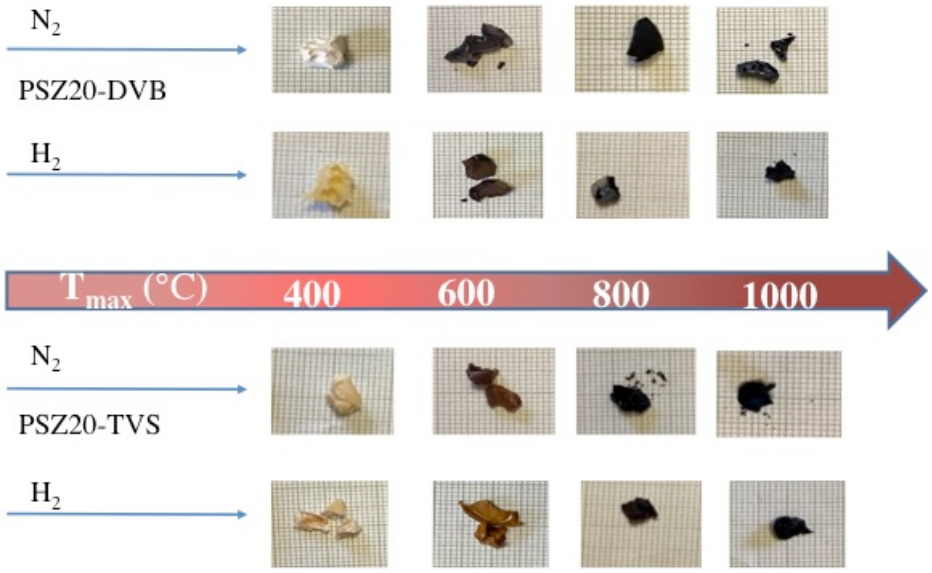

Figure 3.2: Ceramic aerogels of PSZ20-DVB and PSZ20-TVS aerogels pyrolyzed at different temperatures

Although H_2 did not produce a transparent material, it did impact the porosity of the samples. Porosity measurements were conducted on PSZ20-DVB aerogels, using a Micromeritics ASAP 2020 porosity meter. The difference in N_2-sorption isotherms of ceramic aerogels **ca-**H_2 and **ca-**N_2 is noticeable and indicates a higher total adsorbed volume in **ca-**H_2 relative to **ca-**N_2. This is predominantly due to the significantly higher amount of micropores present in **ca-**H_2, as indicated by the sorption behavior at very low pressures. With the shape of both sorption curves quite similar, an almost identical pore size distribution of mesopores is observed. Ultimately, **ca-**H_2 has a more than three-fold larger (BET) surface area than **ca-**N_2.

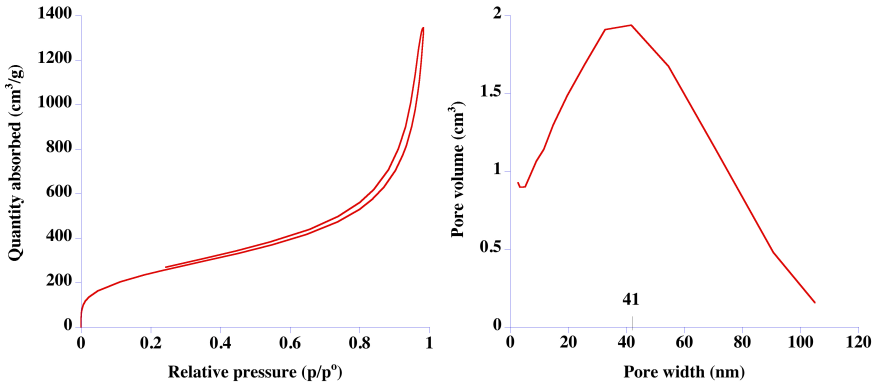

Figure 3.3: N_2-sorption isotherm and pore size distribution (Barrett-Joyner-Halenda (BJH) theory[45]) of the polymeric aerogel, **pa**.

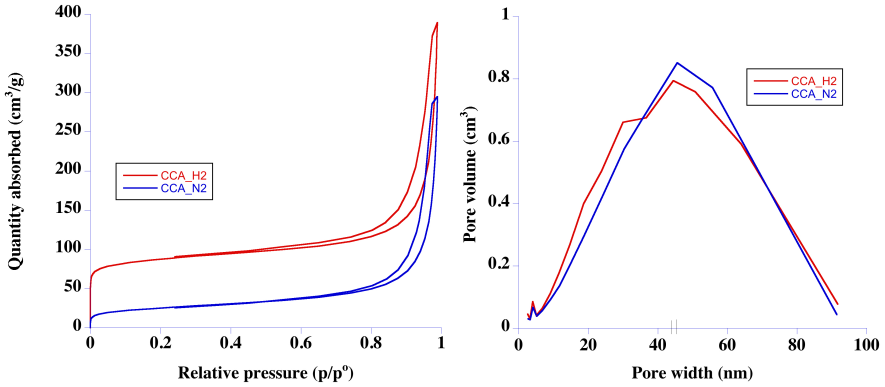

Figure 3.5: N_2-sorption isotherms and BJH pore size distributions of ceramic aerogels, **ca-**H_2 (red) and **ca-**N_2 (blue).

Sample	BET SSA (m^2/g)	Total pore volume (cm^3/g)
Pa	900	2.07
ca-H_2	320	0.58
ca-N_2	95	0.44

Table 3.1: Brunauer–Emmett–Teller (BET[46]) specific surface area (SSA) and total pore volume measured with N_2 adsorption analysis for polymeric aerogel, **pa**, and ceramic aerogels **ca-**H_2 (red) and **ca-**N_2.

In response to the high carbon content of starting material issue, our subsequent endeavor focused on producing an aerogel without any crosslinker. This

required numerous trials and errors, but we eventually succeeded in synthesizing a PSZ20 wet gel without a crosslinker. The process involved mixing 2 gm of Durazane with 6 gm of cyclohexane and adding ~0.03 gm of DCPO as a catalyst. The mixture was stirred for 30 minutes at room temperature before transferring it to a digestion vessel. The vessel was then placed in a preheated oven at 150°C for 6 hours. After cooling down, the gels were extracted from the vessels and rinsed with cyclohexane. Notably, the resulting wet gel exhibited high transparency, which was a significant improvement compared to the previous attempts that utilized crosslinkers.

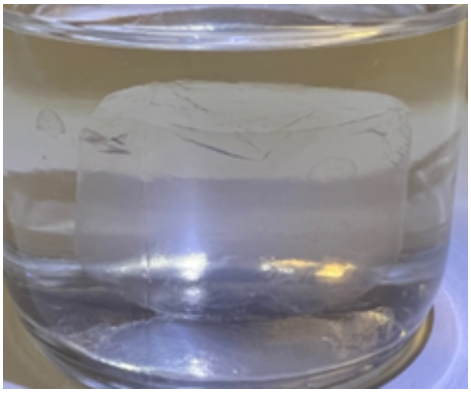

Figure 3.6: Transparent Durazane1800-DCPO-Cyclohexane wet gel

Unfortunately, our progress halted as the supercritical dryer, crucial for the drying process, was not functional. Nevertheless, we remain optimistic about the potential of this route in producing transparent ceramics under a hydrogen atmosphere. With further developments and access to the necessary equipment, we believe this approach holds promise for achieving our goals.

Figure 3.7: Translucency in Durazane1800-DCPO thick films and coatings.

As part of another approach to test our hypothesis, we decided to explore the thin films and coatings instead of bulk materials. Initially, we created a thin layer of Durazane1800-DCPO, approximately 1mm thick, by crosslinking it in a watch glass

in an oven at 150°C for 1 hour. However, the resulting layer broke into pieces, which posed a challenge. Nevertheless, we proceeded with pyrolyzing these small pieces in a hydrogen environment to assess their transparency. Surprisingly, there was not much difference observed between the bulk material and these samples, indicating that transparency was not significantly improved through this method.

Undeterred, we refined our approach and experimented with even thinner layers. This time, we opted for painting a layer of Durazane 1800 on a microscope slide and subsequently pyrolyzing the samples in a furnace at 800°C. These new samples turned out to be fairly transparent compared to the thicker films used previously. This result showed promise in achieving transparency by using thinner coatings, demonstrating a step forward in our research.

Summary

In conclusion, our investigation has provided valuable insights into the complexities of achieving transparent ceramics through pyrolysis. We recognize the importance of further developments, optimization of experimental conditions, and the need for fully functional equipment to continue our pursuit of producing transparent ceramics under a hydrogen atmosphere. Our findings with thinner coatings show promise and open new avenues for exploration in the quest for transparent ceramic materials. With continued dedication and advancements, we believe that our goals of creating transparent ceramics are within reach.

References:

1. Colombo P., R. R., Soraru G., Kleebe, H, , *Historical review of the development of polymer derived cermaics(PDCs). In Polymer Derived Ceramics: From Nanostrcture to Applications*. DEStech Publication Inc.: : 2009; p 1-12.
2. Riedel, R.; Mera, G.; Hauser, R.; Klonczynski, A., Silicon-Based Polymer-Derived Ceramics: Synthesis Properties and Applications-A Review
Dedicated to Prof. Dr. Fritz Aldinger on the occasion of his 65th birthday. *Journal of the Ceramic Society of Japan* **2006,** *114* (1330), 425-444.
3. Colombo, P.; Mera, G.; Riedel, R.; Sorarù, G. D., Polymer-Derived Ceramics: 40 Years of Research and Innovation in Advanced Ceramics. *Journal of the American Ceramic Society* **2010,** *93* (7), 1805-1837.
4. Li, H.; Zhang, L.; Cheng, L.; Wang, Y.; Yu, Z.; Huang, M.; Tu, H.; Xia, H., Effect of the polycarbosilane structure on its final ceramic yield. *Journal of the European Ceramic Society* **2008,** *28* (4), 887-891.
5. Vakifahmetoglu, C.; Zeydanli, D.; Colombo, P., Porous polymer derived ceramics. *Materials Science and Engineering: R: Reports* **2016,** *106*, 1-30.
6. Otitoju, T. A.; Okoye, P. U.; Chen, G.; Li, Y.; Okoye, M. O.; Li, S., Advanced ceramic components: Materials, fabrication, and applications. *Journal of industrial and engineering chemistry* **2020,** *85*, 34-65.
7. Aguirre-Medel, S.; Jana, P.; Kroll, P.; Sorarù, G. D., Towards porous silicon oxycarbide materials: effects of solvents on microstructural features of poly (methylhydrosiloxane)/divynilbenzene aerogels. *Materials* **2018,** *11* (12), 2589.
8. Ionescu, E.; Kleebe, H.-J.; Riedel, R., Silicon-containing polymer-derived ceramic nanocomposites (PDC-NCs): preparative approaches and properties. *Chemical Society Reviews* **2012,** *41* (15), 5032-5052.
9. Choong Kwet Yive, N. S.; Corriu, R. J. P.; Leclercq, D.; Mutin, P. H.; Vioux, A., Silicon carbonitride from polymeric precursors: thermal cross-linking and pyrolysis of oligosilazane model compounds. *Chemistry of Materials* **1992,** *4* (1), 141-146.

10. Scheffler, M., Processing of Ceramics from Polysil(sesquioxane)-Type Precursors: Coatings, Tapes, Tailored Surfaces, and Porosity Control. *Advanced Engineering Materials n/a* (n/a), 2300290.

11. Bahloul, D.; Pereira, M.; Goursat, P.; Yive, N. S. C. K.; Corriu, R. J. P., Preparation of Silicon Carbonitrides from an Organosilicon Polymer: I, Thermal Decomposition of the Cross-linked Polysilazane. *Journal of the American Ceramic Society* **1993,** *76* (5), 1156-1162.

12. Pu, W.; Li, X.; Li, G.; Hu, T., Phenol substituted polymethylsilane: a soluble conducting polymer with low cross-linking density. *Polymer Bulletin* **2015,** *72* (4), 779-790.

13. Nyczyk, A.; Paluszkiewicz, C.; Hasik, M.; Cypryk, M.; Pospiech, P., Cross-linking of linear vinylpolysiloxanes by hydrosilylation–FTIR spectroscopic studies. *Vibrational Spectroscopy* **2012,** *59*, 1-8.

14. Zera, E.; Brancaccio, E.; Tognana, L.; Rivoira, L.; Bruzzoniti, M. C.; Sorarù, G. D., Reactive Atmosphere Synthesis of Polymer-Derived Si–O–C–N Aerogels and Their Cr Adsorption from Aqueous Solutions. *Advanced Engineering Materials* **2018,** *20* (7), 1701130.

15. Strong Jr, K. T.; Arreguin, S. A.; Bordia, R. K., Controlled atmosphere pyrolysis of polyureasilazane for tailored volume fraction Si3N4/SiC nanocomposites powders. *Journal of the European Ceramic Society* **2016,** *36* (15), 3663-3669.

16. Ionescu, E.; Mera, G.; Riedel, R., Polymer-Derived Ceramics (PDCs): Materials Design towards Applications at Ultrahigh-Temperatures and in Extreme Environments. In *Nanotechnology: Concepts, Methodologies, Tools, and Applications*, Management Association, I. R., Ed. IGI Global: Hershey, PA, USA, 2014; pp 1108-1139.

17. Anand, R.; Sahoo, S. P.; Nayak, B. B.; Behera, S. K., Phase evolution, nanostructure, and oxidation resistance of polymer derived SiTiOC ceramic hybrid. *Ceramics International* **2019,** *45* (5), 6570-6576.

18. Francis, A., Progress in polymer-derived functional silicon-based ceramic composites for biomedical and engineering applications. *Materials Research Express* **2018,** *5* (6), 062003.

19. Ackley, B. J.; Martin, K. L.; Key, T. S.; Clarkson, C. M.; Bowen, J. J.; Posey, N. D.; Ponder Jr, J. F.; Apostolov, Z. D.; Cinibulk, M. K.; Pruyn, T. L., Advances in the Synthesis of Preceramic Polymers for the Formation of Silicon-Based and Ultrahigh-Temperature Non-Oxide Ceramics. *Chemical Reviews* **2023,** *123* (8), 4188-4236.

20. Stabler, C.; Ionescu, E.; Graczyk-Zajac, M.; Gonzalo-Juan, I.; Riedel, R., Silicon oxycarbide glasses and glass-ceramics:"All-Rounder" materials for advanced structural and functional applications. *Journal of the American Ceramic Society* **2018,** *101* (11), 4817-4856.

21. Wang, X.; Gao, X.; Zhang, Z.; Cheng, L.; Ma, H.; Yang, W., Advances in modifications and high-temperature applications of silicon carbide ceramic matrix composites in aerospace: a focused review. *Journal of the European Ceramic Society* **2021,** *41* (9), 4671-4688.

22. Lu, D.; Su, L.; Wang, H.; Niu, M.; Xu, L.; Ma, M.; Gao, H.; Cai, Z.; Fan, X., Scalable fabrication of resilient SiC nanowires aerogels with exceptional high-temperature stability. *ACS applied materials & interfaces* **2019,** *11* (48), 45338-45344.

23. Bergero, L.; Sglavo, V. M.; Soraru, G. D., Processing and thermal shock resistance of a polymer-derived MoSi2/SiCO ceramic composite. *Journal of the American Ceramic Society* **2005,** *88* (11), 3222-3225.

24. Sarkar, S.; Zhai, L., Polymer-derived non-oxide ceramic fibers—Past, present and future. *Materials Express* **2011,** *1* (1), 18-29.

25. Yin, X.; Kong, L.; Zhang, L.; Cheng, L.; Travitzky, N.; Greil, P., Electromagnetic properties of Si–C–N based ceramics and composites. *International Materials Reviews* **2014,** *59* (6), 326-355.

26. Pirzada, T. J.; Singh, S.; De Meyere, R.; Earp, P.; Galano, M.; Marrow, T. J., Effects of polymer infiltration processing (PIP) temperature on the mechanical and thermal properties of Nextel 312 fibre SiCO ceramic matrix composites. *Composites Part A: Applied Science and Manufacturing* **2021,** *140*, 106197.

27. Flores, O.; Bordia, R. K.; Nestler, D.; Krenkel, W.; Motz, G., Ceramic fibers based on SiC and SiCN systems: current research, development, and commercial status. *Advanced Engineering Materials* **2014,** *16* (6), 621-636.

28. Bright, V. M.; Raj, R.; Dunn, M. L.; Daily, J. W., Injectable ceramic microcast silicon carbonitride (SiCN) microelectromechanical system (MEMS) for extreme temperature environments with extension: Micro packages for nano-devices. *Colorado University at Boulder Office of Contracts and Grants* **2004**.

29. Ziegler, G.; Kleebe, H.-J.; Motz, G.; Müller, H.; Traßl, S.; Weibelzahl, W., Synthesis, microstructure and properties of SiCN ceramics prepared from tailored polymers. *Materials chemistry and physics* **1999,** *61* (1), 55-63.

30. Andronenko, S. I.; Stiharu, I.; Misra, S. K., Synthesis and characterization of polyureasilazane derived SiCN ceramics. *Journal of Applied Physics* **2006,** *99* (11).

31. Wen, Q.; Yu, Z.; Riedel, R., The fate and role of in situ formed carbon in polymer-derived ceramics. *Progress in Materials Science* **2020,** *109*, 100623.

32. Riedel, R.; Mera, G.; Hauser, R.; Klonczynski, A., Silicon-based polymer-derived ceramics: synthesis properties and applications-a review dedicated to Prof. Dr. Fritz Aldinger on the occasion of his 65th birthday. *Journal of the Ceramic Society of Japan (日本セラミックス協会学術論文誌)* **2006,** *114* (1330), 425-444.

33. Galusek, D.; Reschke, S.; Riedel, R.; Dreßler, W.; Šajgalík, P.; Lenčéš, Z.; Majling, J., In-situ carbon content adjustment in polysilazane derived amorphous SiCN bulk ceramics. *Journal of the European Ceramic Society* **1999,** *19* (10), 1911-1921.

34. Zera, E.; Brancaccio, E.; Tognana, L.; Rivoira, L.; Bruzzoniti, M. C.; Sorarù, G. D., Reactive Atmosphere Synthesis of Polymer-Derived Si–O–C–N Aerogels and Their Cr Adsorption from Aqueous Solutions. *Advanced Engineering Materials* **2018,** *20* (7), 1701130.

35. Narisawa, M.; Funabiki, F.; Iwase, A.; Wakai, F.; Hosono, H., Effects of atmospheric composition on the molecular structure of synthesized silicon oxycarbides. *Journal of the American Ceramic Society* **2015,** *98* (10), 3373-3380.

36. Narisawa, M.; Hokazono, H.; Mitsuhara, K.; Inoue, H.; Ohta, T., Structure and properties of white Si–O–C (–H) ceramics derived from polycarbosilane by thermal oxidation curing and H2 decarbonization process. *Journal of the Ceramic Society of Japan* **2016,** *124* (10), 1094-1099.

37. Dirè, S.; Borovin, E.; Narisawa, M.; Sorarù, G. D., Synthesis and characterization of the first transparent silicon oxycarbide aerogel obtained through H 2 decarbonization. *Journal of Materials Chemistry A* **2015,** *3* (48), 24405-24413.

38. Hu, C.; Sedghi, S.; Silvestre-Albero, A.; Andersson, G. G.; Sharma, A.; Pendleton, P.; Rodríguez-Reinoso, F.; Kaneko, K.; Biggs, M. J., Raman spectroscopy study of the transformation of the carbonaceous skeleton of a polymer-based nanoporous carbon along the thermal annealing pathway. *Carbon* **2015,** *85*, 147-158.

39. Heise, H.; Kuckuk, R.; Ojha, A.; Srivastava, A.; Srivastava, V.; Asthana, B., Characterisation of carbonaceous materials using Raman spectroscopy: a comparison of carbon nanotube filters, single-and multi-walled nanotubes, graphitised porous carbon and graphite. *Journal of Raman Spectroscopy: An International Journal for Original Work in all Aspects of Raman Spectroscopy, Including Higher Order Processes, and also Brillouin and Rayleigh Scattering* **2009,** *40* (3), 344-353.

40. Jorio, A.; Dresselhaus, M. S.; Saito, R.; Dresselhaus, G., *Raman spectroscopy in graphene related systems*. John Wiley & Sons: 2011.

41. Shao, G., Development Of Polymer Derived Sialcn Ceramic And Its Applications For High-temperature Sensors. **2013**.

42. Markel, I. J.; Glaser, J.; Steinbrück, M.; Seifert, H. J., Experimental and computational analysis of PSZ 10-and PSZ 20-derived Si-CN ceramics. *Journal of the European Ceramic Society* **2019,** *39* (2-3), 195-204.

43. Holden, J. M., *Optical properties of C (60) and carbon nanotubes*. University of Kentucky: 1997.

44. Takeda, M.; Saeki, A.; Sakamoto, J.-i.; Imai, Y.; Ichikawa, H., Effect of Hydrogen Atmosphere on Pyrolysis of Cured Polycarbosilane Fibers. *Journal of the American Ceramic Society* **2000,** *83* (5), 1063-1069.

45. Barrett, E. P.; Joyner, L. G.; Halenda, P. P., The determination of pore volume and area distributions in porous substances. I. Computations from nitrogen isotherms. *Journal of the American Chemical society* **1951,** *73* (1), 373-380.

46. Brunauer, S.; Emmett, P. H.; Teller, E., Adsorption of gases in multimolecular layers. *Journal of the American chemical society* **1938,** *60* (2), 309-319.